

Supporting information for

Defect engineering and surface polarization of TiO₂ nanorod arrays toward efficient photoelectrochemical oxygen evolution

Yueying Li^{1, a, *}, Shiyu Liang^{2, a}, Huanhuan Sun², Wei Hua², Jian-Gan Wang^{2, *}

¹ New Energy (Photovoltaic) Industry Research Center, Qinghai University, No. 251 Daning Road, Xining 810016, China

² State Key Laboratory of Solidification Processing, Center for Nano Energy Materials, School of Materials Science and Engineering,

Northwestern Polytechnical University and Shaanxi Joint Lab of Graphene (NPU), No. 127, Youyi West Road, Xi'an 710072, China

^a. These authors contributed equally to this work.

*Corresponding authors: liyy2019@qhu.edu.cn (Y. Li); wangjiangan@nwpu.edu.cn (J.-G. Wang).

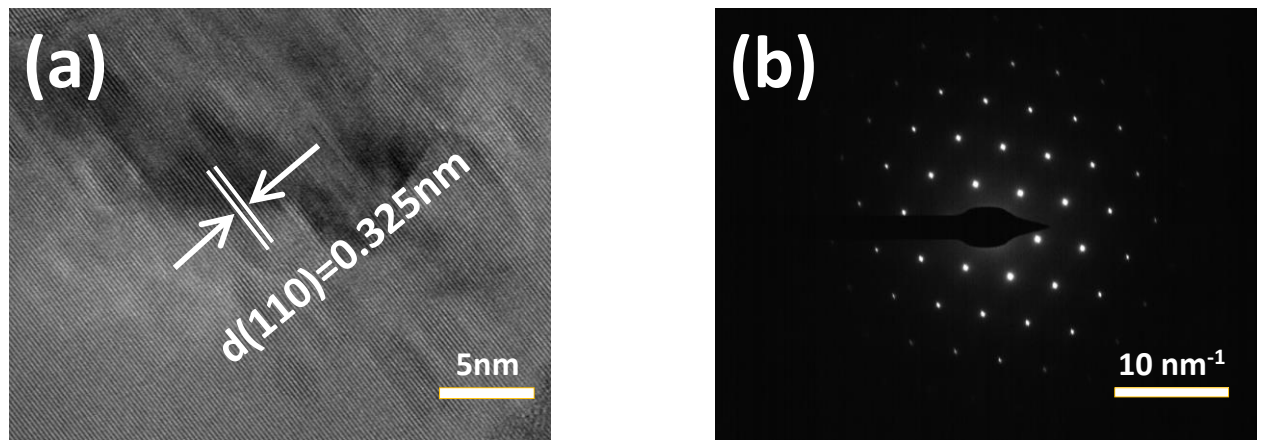


Figure S1. (a) HRTEM and(b) SAED pattern of TiO_2 .

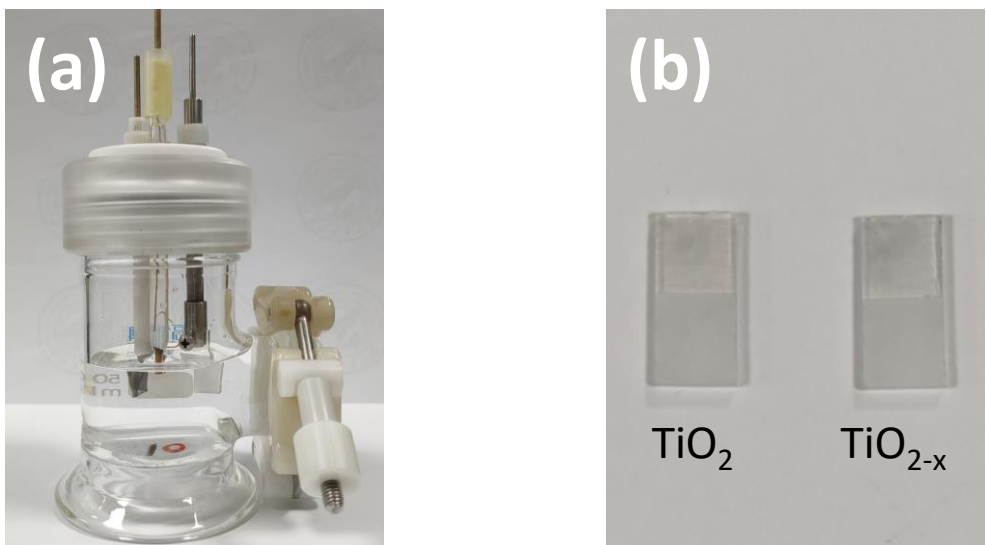


Figure S2. Digital images of (a) the electrochemical cell and (b) as-prepared TiO_2 and TiO_{2-x} samples.

Table S1. Comparison of PEC performance for TiO₂-based photoelectrodes.

Sample	Light source (mW·cm ⁻²)	Electrolyte (pH)	j (mA cm ⁻²) at 1.23 V		Ref.
			Bare	Sample	
TiO ₂ /NH ₂ -MIL(Fe _{0.25} Ni _{0.75})-88	100	0.5M PBS (7)	0.6	1.56	[1]
CQDs/E-TiO ₂	100	0.2 M Na ₂ SO ₄ (7)	0.256	2.55	[2]
UiO-67@TiO ₂	100	1 M KOH (14)	0.5	2.38	[3]
LaCo(OH)x/Au/Sb-TiO ₂	100	0.5 M Na ₂ SO ₄ (7)	0.3	2.0	[4]
Gly-TiO ₂	100	1M NaOH (13.6)	0.6	1.41	[5]
1-Bi/TiO ₂	100	0.05 M PBS (7) 0.35M Na ₂ SO ₃	0.4	1.65	[6]
TiO ₂ /STO/CdS NRs	100	and 0.25 M Na ₂ S (12.5)	0.25	1.85	[7]
NiFe-MOF/TiO ₂	100	0.5 M Na ₂ SO ₄ (6.8)	0.3	0.77	[8]
PCN/Cu-TNA	100	0.2 M Na ₂ SO ₃ (10.2)	0.5	1.42	[9]
r-TiO ₂ /a-TiO ₂ /ZnFe-LDH	100	0.1 M Na ₂ SO ₄ (6.8)	0.73	1.86	[10]
Sn ₃ O ₄ /TiO ₂ /Au	100	0.1 M NaOH (13.6)	0.6	2.5	[11]
TiO _{2-x} NRAs	100	0.2 M Na ₂ SO ₄ (7)	0.81	1.68	[12]
MnO ₂ /N-TiO ₂ NTs	100	1M NaOH (13.9)	0.57	1.95	[13]
VO/Ti-Si-O NTs	100	1 M KOH (13.6)	0.3	1.63	[14]
TiO _{2-x} NTAs	100	1M NaOH (13.9)	0.2	0.73	[15]
TiO _{2-x}	100	1 M NaOH (13.9)	1.5	2.62	This work

Table S2. The fitted values of Nyquist plots according to the equivalent circuit in Figure 5c.

	R_s ($\Omega \text{ cm}^{-2}$)	R_{ct1} ($\Omega \text{ cm}^{-2}$)	R_{ct2} ($\Omega \text{ cm}^{-2}$)
TiO ₂	9.04	139.9	767.5
TiO _{2-x}	5.3	17.48	90.5

References

1. Yoon, J. W.; Kim, J.-H.; Jo, Y.-M.; Lee, J.-H. Heterojunction between bimetallic metal-organic framework and TiO₂: Band-structure engineering for effective photoelectrochemical water splitting, *Nano Research* **2022**.
2. Zhou, T.; Li, L.; Li, J.; Wang, J.; Bai, J.; Xia, L.; Xu, Q.; Zhou, B. Electrochemically reduced TiO₂ photoanode coupled with oxygen vacancy-rich carbon quantum dots for synergistically improving photoelectrochemical performance, *Chem. Eng. J.* **2021**, 425, 131770.
3. Wang, X.; Sun, W.; Tian, Y.; Dang, K.; Zhang, Q.; Shen, Z.; Zhan, S. Conjugated pi electrons of MOFs drive charge separation at heterostructures interface for enhanced photoelectrochemical water oxidation, *Small* **2021**, 17, 2100367.
4. Pal, D.; Sarkar, A.; Ghosh, N. G.; Sanke, D. M.; Maity, D.; Karmakar, K.; Sarkar, D.; Zade, S. S.; Khan, G. G. Integration of LaCo(OH)_x photo-electrocatalyst and plasmonic gold nanoparticles with Sb-doped TiO₂ Nanorods for photoelectrochemical water oxidation, *ACS Appl. Nano Mater.* **2021**, 4, 6111-6123.
5. Ma, W.; Huang, K.; Wu, X.; Wang, M.; Feng, S. Surface polarization enables high charge separation in TiO₂ nanorod photoanode, *Nano Research* **2021**, 14, 4056-4062.
6. Pang, Y.; Zang, W.; Kou, Z.; Zhang, L.; Xu, G.; Lv, J.; Gao, X.; Pan, Z.; Wang, J.; Wu, Y. Assembling of Bi atoms on TiO₂ nanorods boosts photoelectrochemical water splitting of semiconductors, *Nanoscale* **2020**, 12, 4302-4308.
7. He, Y.; Zhu, J.; Yuan, Y.; Li, M.; Yang, Y.; Liu, Y.; Chen, M.; Cao, D.; Yan, X. Dual-regulation charge separation strategy with the synergistic effect of 1D/0D heterostructure and inserted ferroelectric layer for boosting photoelectrochemical water oxidation, *J. Mater. Chem. A* **2021**, 9, 7594-7605.
8. Cui, W.; Bai, H.; Shang, J.; Wang, F.; Xu, D.; Ding, J.; Fan, W.; Shi, W. Organic-inorganic hybrid-photoanode built from NiFe-MOF and TiO₂ for efficient PEC water splitting, *Electrochim. Acta* **2020**, 349, 136383.
9. Wang, L.; Si, W.; Ye, Y.; Wang, S.; Hou, F.; Hou, X.; Cai, H.; Dou, S. X.; Liang, J. Cu-Ion-Implanted and Polymeric Carbon Nitride-Decorated TiO₂ Nanotube Array for Unassisted Photoelectrochemical Water Splitting, *ACS Appl. Mater. Interfaces* **2021**, 13, 44184-44194.
10. Zhang, S.; Liu, Z.; Chen, D.; Guo, Z.; Ruan, M. Oxygen vacancies engineering in TiO₂ homojunction/ZnFe-LDH for enhanced photoelectrochemical water oxidation, *Chem. Eng. J.* **2020**, 395, 125101.
11. Dong, G.; Cheng, X.; Bi, Y. Hierarchical TiO₂ photoanodes with spatial charge separation for efficient oxygen evolution reaction, *Solar RRL* **2020**, 5, 2000449.
12. Huang, C.; Bian, J.; Guo, Y.; Huang, M.; Zhang, R.-Q. Thermal vacuum de-oxygenation and post oxidation of TiO₂ nanorod arrays for enhanced photoelectrochemical properties, *J. Mater. Chem. A* **2019**, 7, 5434-5441.
13. Cheng, X.; Dong, G.; Zhang, Y.; Feng, C.; Bi, Y. Dual-bonding interactions between MnO₂ cocatalyst and TiO₂ photoanodes for efficient solar water splitting, *Appl. Catal. B: Environ.* **2020**, 267, 118723.
14. Dong, Z.; Cai, Y.; Zhang, K.; Chu, Z.; Han, S.; Li, Z. Electrochemical reduction induced self-doping of oxygen vacancies into Ti-Si-O nanotubes as efficient photoanode for boosted photoelectrochemical water splitting, *Int. J. Hydrogen Energy* **2021**, 46, 3554-3564.
15. Kang, Q.; Cao, J.; Zhang, Y.; Liu, L.; Xu, H.; Ye, J. Reduced TiO₂ nanotube arrays for photoelectrochemical water splitting, *J. Mater. Chem. A* **2013**, 1, 5766-5774.